A GCM Study of Tropical–Subtropical Upper-Ocean Water Exchange

ZHENGYU LIU AND S. G. H. PHILANDER,

UCAR Visiting Scientist Program, Program in Atmospheric and Oceanic Sciences, Princeton University, Princeton, New Jersey

R. C. PACANOWSKI

GFDL/NOAA, Princeton University, Princeton, New Jersey

(Manuscript received 5 March 1993, in final form 7 June 1994)

ABSTRACT

Experiments with an oceanic general circulation model indicate that the tropical and subtropical oceanic circulations are linked in three ways. Far from coasts in the oceanic interior, equatorial surface waters flow poleward to the southern part of the subtropical gyre, and then are subducted and returned in the thermocline to the upper part of the core of the Equatorial Undercurrent. There is, in addition, a surface western boundary current that carries waters from the equatorial region to the northern part of the subtropical gyre. After subduction, that water reaches the equator by means of a subsurface western boundary current and provides a substantial part (2/3 approximately) of the initial transport of the Equatorial Undercurrent. The eastward flow in the Equatorial Undercurrent is part of an intense equatorial cell in which water rises to the surface at the equator, drifts westward and poleward, then sinks near 3° latitude to flow equatorward where it rejoins the undercurrent.

1. Introduction

Although there have been numerous studies of the subtropical oceanic circulation [see Rhines (1986) and Pedlosky (1991) for reviews] and of the oceanic circulation of the upper equatorial oceans [see McCreary (1985) and Philander (1990) for reviews], little attention has been paid to the links between the equatorial and subtropical circulations. Information about these links is available from hydrographic and direct measurements in the Pacific, which show that a substantial portion of water in and below the Equatorial Undercurrent is supplied from the south by a narrow coastal western boundary current, which can be traced back to the extratropics (Tsuchiya et al. 1989). Isopycnal analysis of salinity and other tracers (Tsuchiya 1981) indicates that the 13°C mode water below the equatorial thermocline of the eastern Pacific can be traced back to the surface layers near New Zealand. Toggweiler et al. (1989) point out that the origin of this water can be traced further to the Circumpolar Current and to the waters off Peru near the equator.

These observations suggest that the upper equatorial and the subtropical oceans are connected both in the oceanic interior and along the western boundary. Pedlosky (1987) proposed a model in which subducted extratropical surface water reaches the equatorial region where it joins the Equatorial Undercurrent. McCreary and Yu (1992) and Liu (1994) obtain similar results and discuss the physical mechanisms that effect the latitudinal exchange of mass.

In this paper we continue to investigate the links between the Tropics and subtropics by means of oceanic GCM experiments. We pay particular attention to the three-dimensional structure of the flow and show that incorrect inferences can be drawn from results for the streamfunction, a two-dimensional field. The paper is arranged as follows. Section 2 introduces the model and the experiments to be performed; section 3 studies the mass exchange as inferred from the flow and transport fields. In section 4, particle trajectories are used to further study the three-dimensional structure of the water exchange. We will trace water that is subducted in the subtropics to the equatorial region and then turn to the trajectories of water parcels that flow from the equatorial region toward the subtropics. In section 5, we attempt to identify the origin of the Equatorial Undercurrent. Section 6 summarizes the results.

2. The model and the experiments

The method of solution for the equations is that of Bryan (1969) as implemented in the GFDL MOM code (Pacanowski et al. 1991). The domain is an idealized rectangular basin from 40°S to 40°N in latitude and from 0° to 60° in longitude, with a flat bottom at 3000 m. The longitudinal resolution is 1°; the latitudinal resolution is 1/3° within 6° of the equator and increases

Corresponding author address: Zhengyu Liu, Department of Atmospheric and Oceanic Sciences, 1225 W. Dayton St., University of Wisconsin—Madison, Madison, WI 53706.
E-mail: znl@ocean.meteor.wisc.edu

linearily to 1° at the domain boundaries on 40°. There are 30 levels in the vertical with a 10-m resolution in the top 100 m.

Horizontal mixing is the constant coefficient scheme with the eddy viscosity and diffusivity of 2×10^7 and 10^7 cm^2 s^{-1} respectively. In two sponge layers, poleward of 35°, temperature is restored to prescribed values with a restoring timescale of 40 days at 35°. This value decreases to 4 days at 40°. The eddy viscosity for momentum equations increases linearly to 2×10^8 cm^8 s^{-1} from 35° to 40°. In the vertical, a Richardson number–dependent scheme is used (Pacanowski and Philander 1981). Unstable temperature gradients are eliminated by mixing heat vertically to a depth that ensures a stable density gradient.

The initial condition is a state of rest. Salinity remains at a constant value of 35 psu. The initial temperature is prescribed [as shown in Fig. 1 of Liu and Philander (1994)]. It is zonally independent and symmetric about the equator. The initial temperature profile on the surface is also used to restore the surface temperature with a 40-day relaxation time. Poleward of 35° this temperature profile is also used as boundary restoring values in the sponge layers.

Three experiments will be discussed in this paper. The forcing and initial condition are symmetric about the equator in all cases but the winds change as shown in Fig. 1. In the first two cases (Fig. 1a,b), the wind stress patterns are unrealistic. In the first (Fig. 1a), easterly winds are "uniform" (no curl) so that the subtropical circulation is unrealistic. The second case (Fig. 1b) has no winds near the equator, but westerly winds with negative curl beyond 5°. In the third control run, the reasonably realistic wind stress consists of two parts: a "uniform" easterly wind within 12° of the equator and a subtropical wind with a negative curl between 12° and 35° (see Fig. 1c). Except for the second case, the experiments are integrated for 17 years after which the temperature still exhibits a slowly varying trend, presumably due to the deep thermohaline spinup process. However, long before this time, the thermocline temperature field is in a quasi-equilibrium state in both the equatorial and subtropical regions. The case with no easterly winds was integrated for 7 years with the initial state corresponding to the control run at year 13. The results shown are averages for the last six months of each run.

3. Flow field

a. Intergrated circulation

The vertically intergrated transports are presented in the left panels of Fig. 1. Outside the equatorial band (>5°), the transport agrees well with Sverdrup theory. In the case with easterly winds, the absence of any curl means that there is no barotropic circulation in the extratropics (Fig. 1a). In the other two cases the negative curl forces well-defined subtropical gyres (Fig. 1b,c). The coarse longitudinal resolution of the model causes the western boundary currents to be viscous in comparison with those in reality. The circulation therefore resembles that of Munk (1950).

"Uniform" easterly winds (Fig. 1a) drive, within 5° of the equator, two counter-rotating gyres that share an eastward current along the equator. Each has a transport of about 5.5 Sv (Sv $\equiv 10^6$m^{3}s^4). Such gyres, which are established after a few months and include the subsurface Equatorial Undercurrent, have previously been studied by Philander and Pacanowski (1980) and Semtner and Holland (1980).

The currents near the equator depend primarily on the winds near the equator. In the absence of any equatorial winds (Fig. 1b), there is no Equatorial Undercurrent. If, on the other hand, the equatorial winds remain unaltered while those in the subtropics are changed, as in Fig. 1c, the equatorial gyre remains practically the same, with only a slight increase in the transport (to about 6.3 Sv). None of the three cases has any barotropic circulation between the equatorial and the subtropical gyres—a consequence of the zero wind stress curl between the gyres. The horizontal gyres are therefore not associated with any mass exchange. However, the meridional circulation can cause such an exchange because the surface poleward Ekman drift has to be returned southward in the subsurface. Figure 2 shows meridional streamfunctions. The case with pure easterly winds (Fig. 2a) has, in each hemisphere, a strong equatorial cell within 5° of the equator in the upper 100 m. (Hereafter, we will use "cell" to refer to the zonally integrated meridional circulation, and "gyre" for the vertically integrated horizontal circulation.) This equatorial cell [which is similar to that of McCreary and Lu (1994)] is associated with strong upwelling on the equator, divergent flow at the surface, downwelling between 3° to 5°, and subsurface flow that converges on the equator. Its meridional extent coincides with that of the equatorial gyre (Fig. 1a).

In the extratropics, winds with no curl induce a slow, broad cell with a descending branch that extends all the way to midlatitudes. The flow is equatorward at depths between 100 and 200 m. Water wells up at the equator and flows poleward by means of Ekman drift associated with the easterly wind. This cell is similar to the subtropical cell of McCreary and Lu (1994), and has been observed in many GCM experiments.

Figure 2b shows that, in the absence of equatorial winds, the connection between the subtropics and the equatorial region is essentially cut off. The subducted subtropical water flows equatorward at depth, rises to the surface north of the region where the winds vanish, and returns poleward as surface Ekman drift.

Figure 2c shows that easterly winds in the Tropics that have a curl in the subtropics drive a circulation that amounts to a combination of those in Figs. 2a and 2b. The local equatorial cell is similar to that in Fig. 2a except for being somewhat deeper. The subtropical

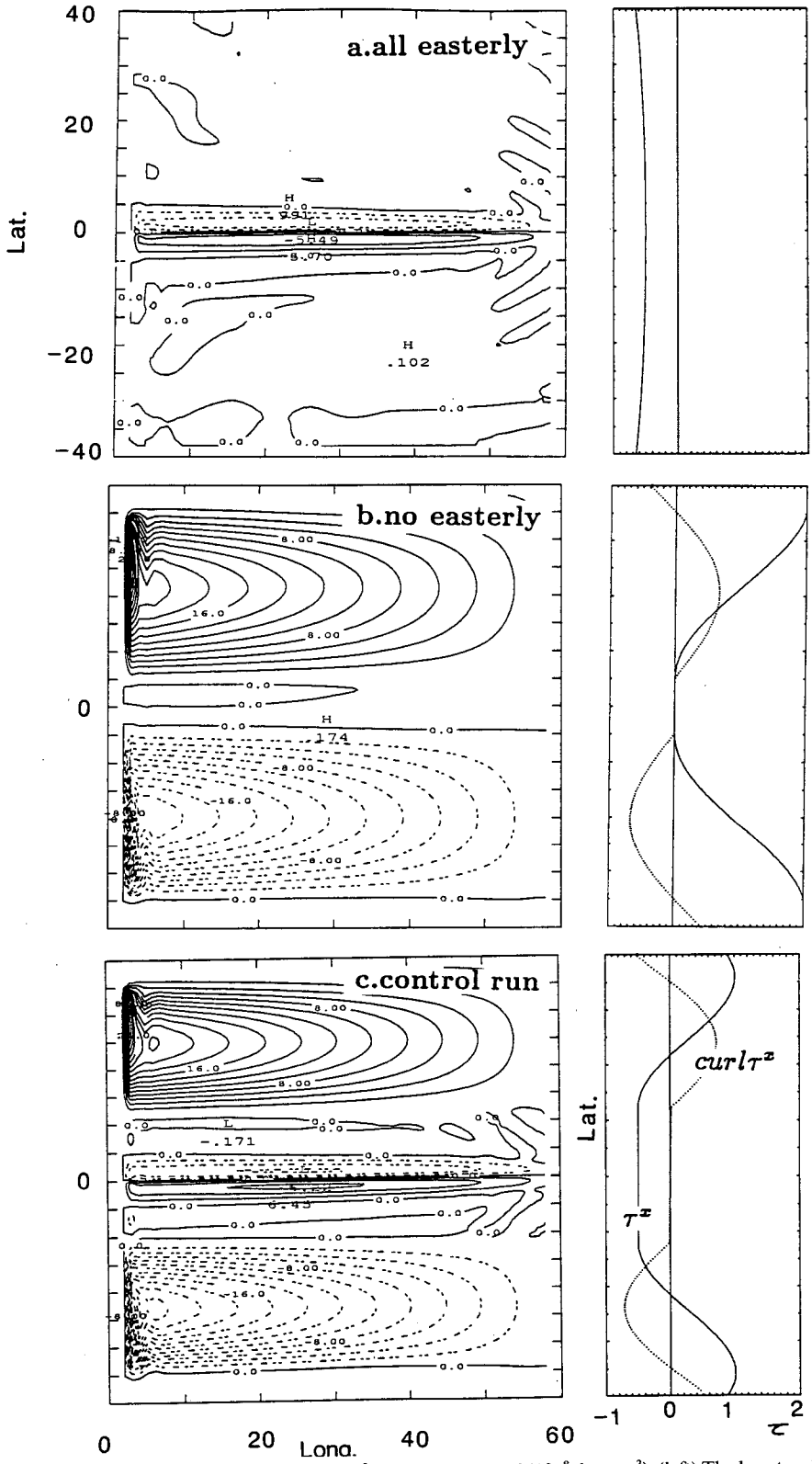

FIG. 1. (right) The wind stress (dyn cm^{-2}) and the wind curl (10^{-8} dyn cm^3). (left) The barotropic streamfunction (Sv). (a) Easterly wind case, only the equatorial gyre exists. (b) Westerly wind case, only the subtropical gyre exists. (c) Control run, both a subtropical gyre and an equatorial gyre exist in each hemisphere.

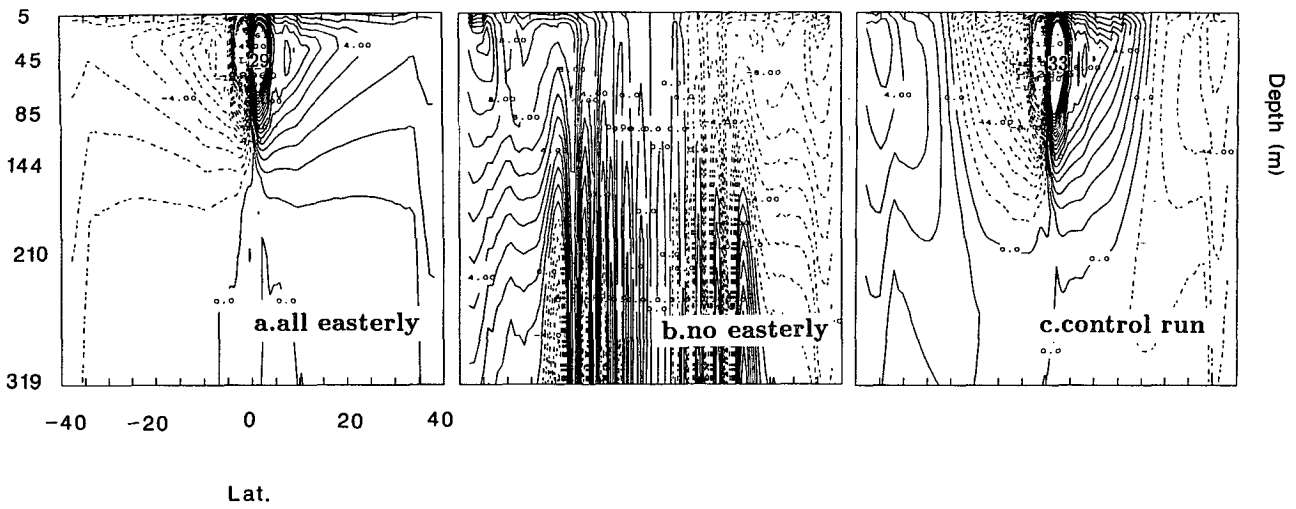

FIG. 2. The meridional streamfunction (contour interval: 1 Sv). (a) Easterly winds drive an equatorial cell and subtropical cell. (b) Westerly winds that drive a subpolar cell. (c) Control run with equatorial cell, subtropical cell, and subpolar cell. Counter intervals above 20 Sv are not plotted.

cell, which connects the equatorial and the subtropical region, now extends poleward to the middle of the subtropical gyre where the surface easterly wind vanishes. The subtropical cell should be called the easterly subtropical cell, because the cell exists only beneath easterly wind.[1] The transport of the subtropical cell is about 7 Sv in the case with only easterly winds and about 8 Sv in the control run. Thus the curl of the subtropical winds has little effect on the exchange. Liu (1993) explains how the transport is determined mainly by the easterly wind at the southern boundary of the subtropical gyre.

The meridional transport of the subtropical cell is approximately 25% of the equatorial cell. This result, which is consistent with those of McCreary and Yu (1992), seems to suggest that most of the water in the Equatorial Undercurrent comes from the equatorial region. However, as will be seen later, this is an incorrect inference because the equatorial cell involves the rapid recirculation of a relatively small amount of water. We return to this matter later.

Although the subtropical cell appears to flow in the same direction as the equatorial cell, there are several obvious differences between the two cells. First, the descending branch of the subtropical cell is far broader and slower than the equatorial cell. Second, the descending branch of the subtropical cell is separated from that of the equatorial cell by weak upwelling near approximately 5° latitude. This can clearly be observed in the velocity field and is also in the transport field in Figs. 2a,c. Third, the physical mechanisms for the two cells are different. The equatorial cell is determined by equatorial dynamics. The subtropical cell is driven by the poleward Ekman drift under the easterly winds with the descending branch located in the region of downward Ekman pumping.

It is now clear that the subtropical cell contributes significantly to the mass exchange between the equatorial and subtropical regions. However, the 2D meridional streamfunction in Fig. 2c seems to suggest that the equatorial region is connected only to the southern subtropical gyre (of the Northern Hemisphere), but not to the northern subtropical gyre where the surface Ekman flux is southward. This turns out to be another misleading feature of the 2D streamfunction. The surface flow (not shown) indicates penetration of equatorial water to the northern part of the subtropical gyre through the surface western boundary current. This water has to return southward, a matter to which we return later.

b. Isothermal analysis

Figure 3 shows streamlines on three isothermal surfaces, those of $T = 22.5°C$, 19°C, and 15.5°C.[2]

The 19°C isotherm lies near the middle of the equatorial thermocline. The 22.5°C and 15.5°C isotherms are located above and below the equatorial thermo-

[1] Farther poleward, the meridional circulation resembles that in the Fig. 2b, with surface water flowing equatorward and returning back at depth mostly within the subtropics. This cell contributes little to the subtropical–equatorial mass exchange (less than 1 Sv) and therefore will not be discussed.

[2] Calculations show that in the interior of the ocean the entrainment vertical velocity is much smaller than the vertical velocity in the subsurface, particularly in the equatorial region. Thus a velocity field on an isopycnal surface represents real particle trajectories much better than does a horizontal velocity.

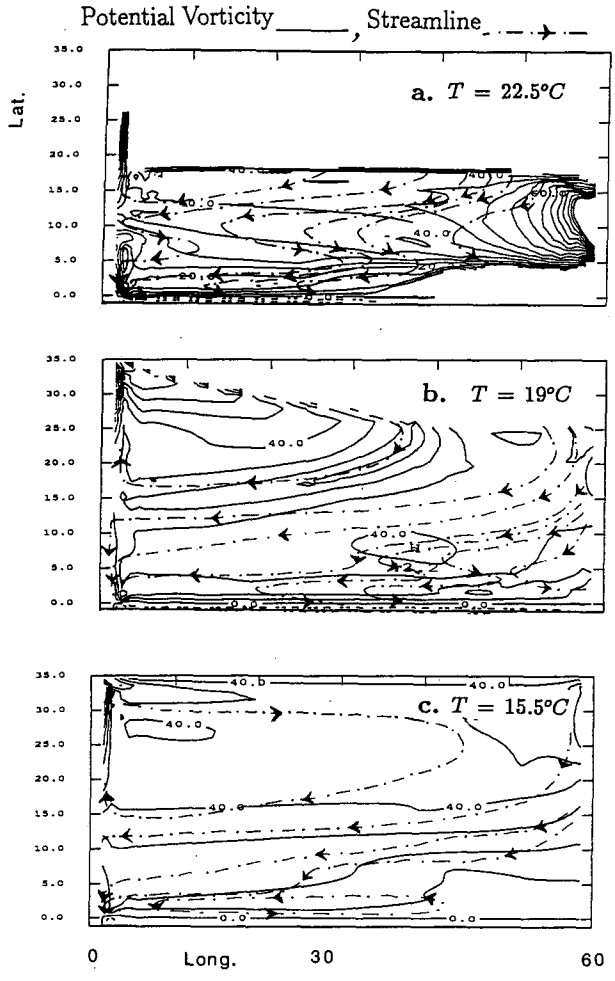

FIG. 3. Potential vorticity and streamlines on isothermal surfaces: (a) $T = 22.5°C$ ($\sigma = 23.8$)--a, (b) $T = 19°C$ ($\sigma = 24.8$)--a 1, (c) $T = 15.5°C$ ($\sigma = 25.6$)--, a deep unventilated isopycnal. Two types of subtropical-equatorial exchange streamlines are present in (a) and (b), both subducting in the eastern subtropical gyre. One type reaches the western boundary first and then flows equatorward through the low-latitude western boundary current. The other type penetrates equatorward from the interior.

cline, respectively (see Fig. 12). Potential vorticity is almost conserved on the 19°C surface within the subtropical gyre (but not in the equatorial region). This is indicative of ventilation processes. The shallow 22.5°C surface is strongly influenced by the surface detrainment process so that potential vorticity is not conserved.

On the 19°C surface (see Fig. 4c), there are three types of subduction streamlines. The first type subducts in the western and central part of the outcrop line—this is known as the recirculation window—and then recirculates within the subtropical gyre. The second type subducts east of the first type. After intersecting the western boundary, the flow is equatorward. The third type of streamline, found further east, also penetrates toward the equator but by means of a zig-zag path in the oceanic interior. The latter two types of streamlines represent two flow patterns for mass exchange: through the western boundary current and through the oceanic interior. Thus, the subduction region for these streamlines is called the "subduction exchange window." More specifically, the second type of streamlines starts from the western boundary exchange window, whereas the third type subducts from the interior exchange window (Liu 1993). On the middle 19°C surface (Fig. 3b) it is obvious that the water exchange is dominated by streamlines through the western boundary.

The shallow 22.5°C surface also has three types of streamlines. However, the water exchange occurs primarily through the interior of the ocean. The streamlines tend to be more eastward than those on the middle 19°C surface. This is consistent with the β spiral structure under downward Ekman pumping. In addition, if water subducts in the very eastern part, it surfaces

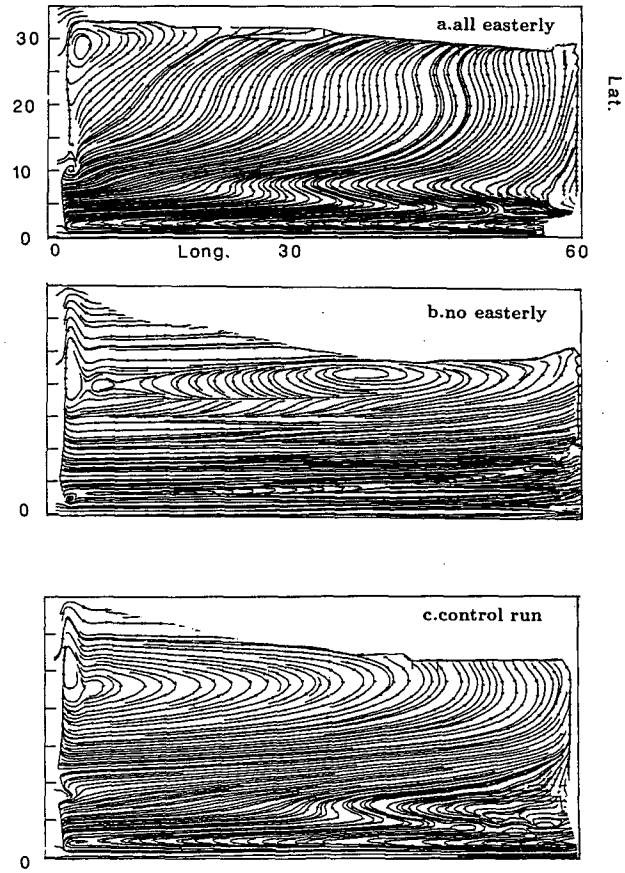

FIG. 4. The streamlines of subducted water on the isothermal surface $T = 19°C$ in (a) the case with easterly winds, (b) the case with westerly winds, and (c) the control run. Note that (a) has a wide mass exchange window, (b) has essentially none, and (c) has a moderate one. (These streamlines connect the horizontal velocity vectors on the isopycnal and thus are not genuine streamlines.)

before reaching the equator, because the cold tongue in the eastern equatorial ocean forces a shallow isopycnal to outcrop outside the equatorial region. Below the main thermocline in the deep 15.5°C surface, there is essentially no water exchange between the subtropics and the equatorial region.

The water subducted in the southern part of the subtropical gyre tends to flow equatorward through the oceanic interior (Fig. 3a). This flow corresponds to the subtropical cell in Fig. 2c.

The northern subtropical gyre receives equatorial water through the surface western boundary current. The return flow to the equatorial region occurs predominantly through the subsurface low-latitude western boundary current (Fig. 3b). This water is masked in the meridional streamfunction field Fig. 2c. These two flow patterns will be confirmed later in the trajectory analysis.

Figure 4 presents the streamline field on $T = 19°C$ for the three runs. The case with strictly easterly winds, which force downward Ekman pumping, has southward thermocline flow. In the case with no easterly winds the flow is almost zonal in the region north of the equator. It intersects the western boundary and returns northward through the midlatitude western boundary current. This case has a very weak mass exchange between the Tropics and subtropics through the low-latitude western boundary current. In comparison with the control run in Fig. 4c, it is apparent that the case with strictly easterly winds has a much wider mass exchange window, whereas the case with no easterly winds has essentially no mass exchange window. This is consistent with the theory of Liu (1994), who shows that the size of the mass exchange window (ΔX) is proportional to the strength of the easterly wind at the southern boundary of the subtropical gyre (τ_{SB}), but is inversely proportional to the strength of the Ekman pumping within the subtropical gyre (w_e); that is,

$$\Delta X(y) \sim \tau_{SB}/w_e(y), \tag{3.1}$$

where y is a latitude in the subtropical gyre. The weak downward Ekman pumping in the case with only easterly winds produces very weak subduction velocities. Thus, to accomplish the mass exchange, a much wider window is needed as shown in Fig. 4a. The absence of easterlies requires no mass exchange, and hence no mass exchange window in the subtropical gyre.

c. *The velocity field*

Figures 5a–d present the velocity field on four zonal sections. In the section through the subtropical gyre (Fig. 5d) the interior is filled with southward Sverdrup flow that has a barotropic structure. The flow returns in the midlatitude western boundary current. The interior flow downwells because of the Ekman pumping, and is eastward because of the westerly winds at that latitude.

Figures 5a–c, sections that are south of the subtropical gyre, have qualitative similarities and differ significantly from Fig. 5d, the section through the subtropical gyre. First of all, the meridional flow has a baroclinic structure; it is poleward through the surface Ekman layer and equatorward in the subsurface. This feature is most pronounced near the equator at 3.3° latitude in Fig. 5a.

Second, the meridional flow has a tendency for western boundary intensification that is much weaker than that in the subtropics. In Fig. 5d the velocity of the midlatitude western boundary current is about 50 times larger than that in the interior. South of the subtropical gyre in Figs. 5a–c the velocity of the low-latitude western boundary current is no more than 10 times that of the interior velocity.

Third, in the oceanic interior, water tends to flow eastward near the surface, westward at depth (Figs. 5b,c). Near the equator, the interior zonal flow is westward at all depths (Fig. 5a). This is also consistent with the isothermal analysis in Fig. 4.

Finally, as seen in Figs. 5b and 5c, the winds cause the isotherms to shoal in an eastward direction. This implies a southward geostrophic flow in the upper ocean. Within the surface Ekman layer, this geostrophic component will decrease the Ekman drift. Thus, one should expect the northward surface transport to be smaller than the Ekman transport.

d. *Subtropical–tropical mass exchange*

In Fig. 6, the positive and negative solid lines are, respectively, the total northward and southward transports, calculated by intergrating the northward and southward velocities separately (so that there is no cancellation). The first feature is the almost complete compensation between the total northward and southward transports in the upper 320 m. The net transport (the light dotted line) is less than 1 Sv.

The second feature is the structure of the total northward (southward) transport: it has two maxima (in the subtropical and equatorial regions, respectively) and a minimum in between. The maximum in the subtropics corresponds to the subtropical gyre as presented in Fig. 1. The return flow is in the western boundary current. This is seen clearly from the dash–dot curve, which is the total northward (or southward) transport within 5° of the western boundary. In the subtropical region the total northward transport is almost identical to the total western boundary northward transport. It follows that cancellation of the total northward and southward transports in the subtropical gyre simply represents the horizontal circulation as shown in the barotropic stream function in Fig. 1.

The maximum in the equatorial region has two contributors: the barotropic, horizontal equatorial gyre and

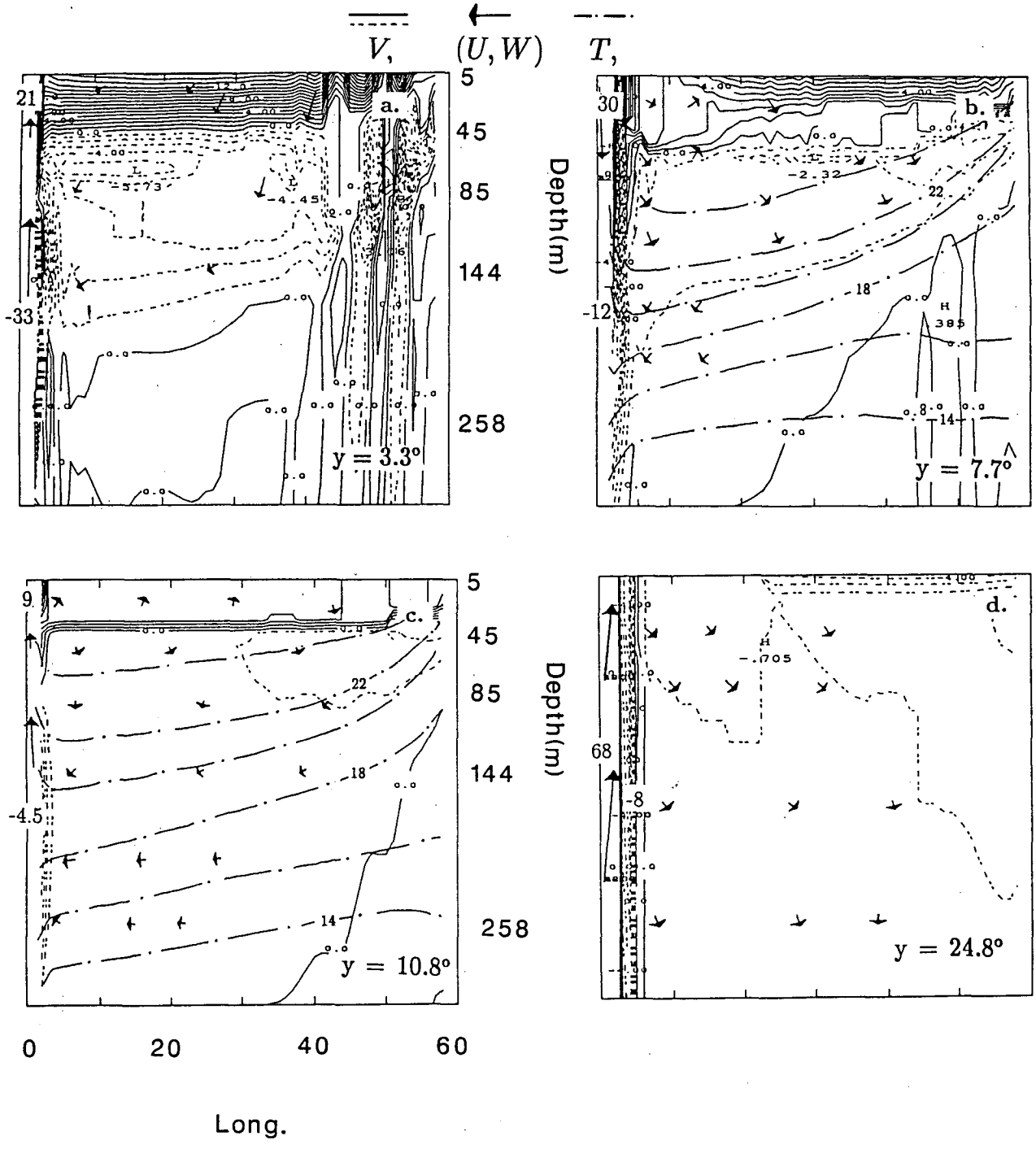

FIG. 5. Zonal sections that show the meridional velocity and the (u,w) velocity vectors: (a) $y = 3.3°$, (b) $y = 7.7°$, (c) $y = 10.8°$, and (d) $y = 24.8°$. The meridional velocity is positive for solid lines and negative for dashed lines with a contour interval of 1 cm s^{-1}. Contour values beyond ± 20 cm s^{-1} are not drawn. Isotherms (dash–dotted line) are drawn in (b) and (c) with a contour interval of 2°. The northward surface flow and the southward subsurface flow are evident south of the subtropical gyre in (a)–(c).

the vertical equatorial cell. The maximum total northward (southward) transport in the equatorial region is 38 Sv, which is approximately the sum of the equatorial cell (25 Sv) and the equatorial gyre (6.5 Sv). Unlike the subtropical gyre, the equatorial circulation (both the equatorial gyre and equatorial cell) is limited to shallow layers. The total transport in the upper 320 m includes all the transport of the equatorial gyre and

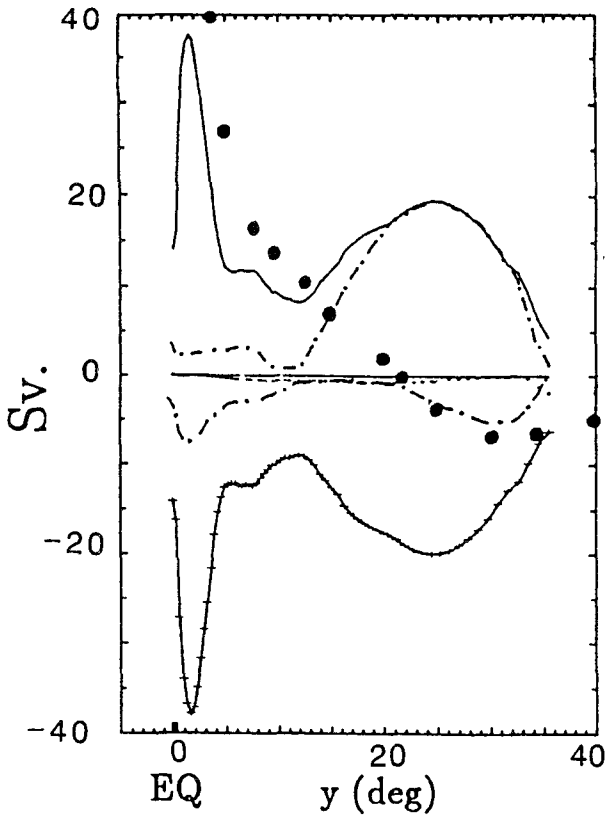

FIG. 6. The total northward (positive) and southward (negative) meridional transport (solid lines) in the top 320 m. The net transport (light dotted curve) is practically zero because the northward and southward transports in the upper 320 m cancel. The total western boundary northward and southward transports (within 5° of the western boundary) are drawn as dash-dotted lines. The heavy dots represent the Ekman transport.

equatorial cell. Thus, the compensation of the total transport in the equatorial region is due to the vertically circulating equatorial cell, and to a lesser extent, due to the horizontally circulating equatorial gyre.

The total northward transport has a minimum of 7 Sv at the southern boundary of the subtropical gyre 12°N. (The minimum transport occurs here because, toward the south, the Ekman transport and the compensating flow increase, toward the north, the barotropic Sverdrup flow due to the wind curl also increases the meridional transport.) It is this transport that represents the subtropical–tropical mass exchange. This surface northward flow (as seen in Figs. 5b,c) almost balances the subsurface return flow.

Furthermore, the western boundary total transports, for both surface northward and subsurface southward flow, are 20% less than the total transport south of the subtropical gyre. Thus, as expected from Figs. 5a–c, the meridional transport between the subtropics and the equatorial region is dominated by interior transport. However, this does not mean that mass exchange between the subtropical gyre and the Equatorial Undercurrent occurs mainly in the interior of the ocean. We will return to this point in later sections.

Finally, the exchange transport at the southern boundary is about 15% less than the Ekman transport (heavy dotted curve). The reason is the surface northward geostrophic flow in the oceanic interior (Figs. 5b,c).

4. Mass exchange: A trajectory analysis

At the beginning of year 17, many particles are released at different locations in the basin. The following figures show their trajectories.

a. Equatorward flow of subtropical water

1) SUBDUCTION PARTICLE TRAJECTORIES

To see the path of the subducted water clearly, we plot, in Fig. 7, three groups of trajectories, that start on the surface in the northern subtropical gyre (at 26°N). Each group has 100 particles, which are distributed randomly within a 3° × 3° area. Figure 7a shows the 3D plot for the group starting from the midbasin, while Fig. 7b shows the top view. Most particles are seen to return northward along the midlatitude western boundary current. They recirculate in the subtropical gyre except for a few that flow equatorward through the low-latitude western boundary current.

Figures 7c and 7d depict another group of particles that starts to the east along 10°. In contrast to those in Figs. 7a,b, all particles now penetrate far south, mostly through the low-latitude western boundary current. After traveling through the Equatorial Undercurrent, some particles return back to the northern subtropics through the surface wind drift and western boundary current. The last group starts 10° farther east as shown in Figs. 7e,f. All particles approach the equator but, unlike those in Figs. 7c,d, the particles reach the equator through the interior of the ocean.

The three types of flow path are consistent with the isothermal analysis in Fig. 3b and Fig. 4c. They can be summarized as in Fig. 8a, which shows three typical trajectories, one for each group. Figure 8c depicts the time history of the temperature and depth of each particle. In the first year, particles are in the surface mixed layer. As they drift southward in the Ekman layer the temperature of each particle increases. From year 1 to year 4, particles subducted in the permanent thermocline move downward, because of strong Ekman pumping within the subtropical gyre, while remaining at the same temperature. Thus the subduction process within the subtropical gyre is predominantly adiabatic. After year 4, particle A joins the midlatitude western boundary current. Particles B and C approach the southern boundary of the subtropical gyre. Figure 8c shows that the temperatures of particles B and C increase while they move downward. After year 7, particles B and C join the rapid equatorial circulation.

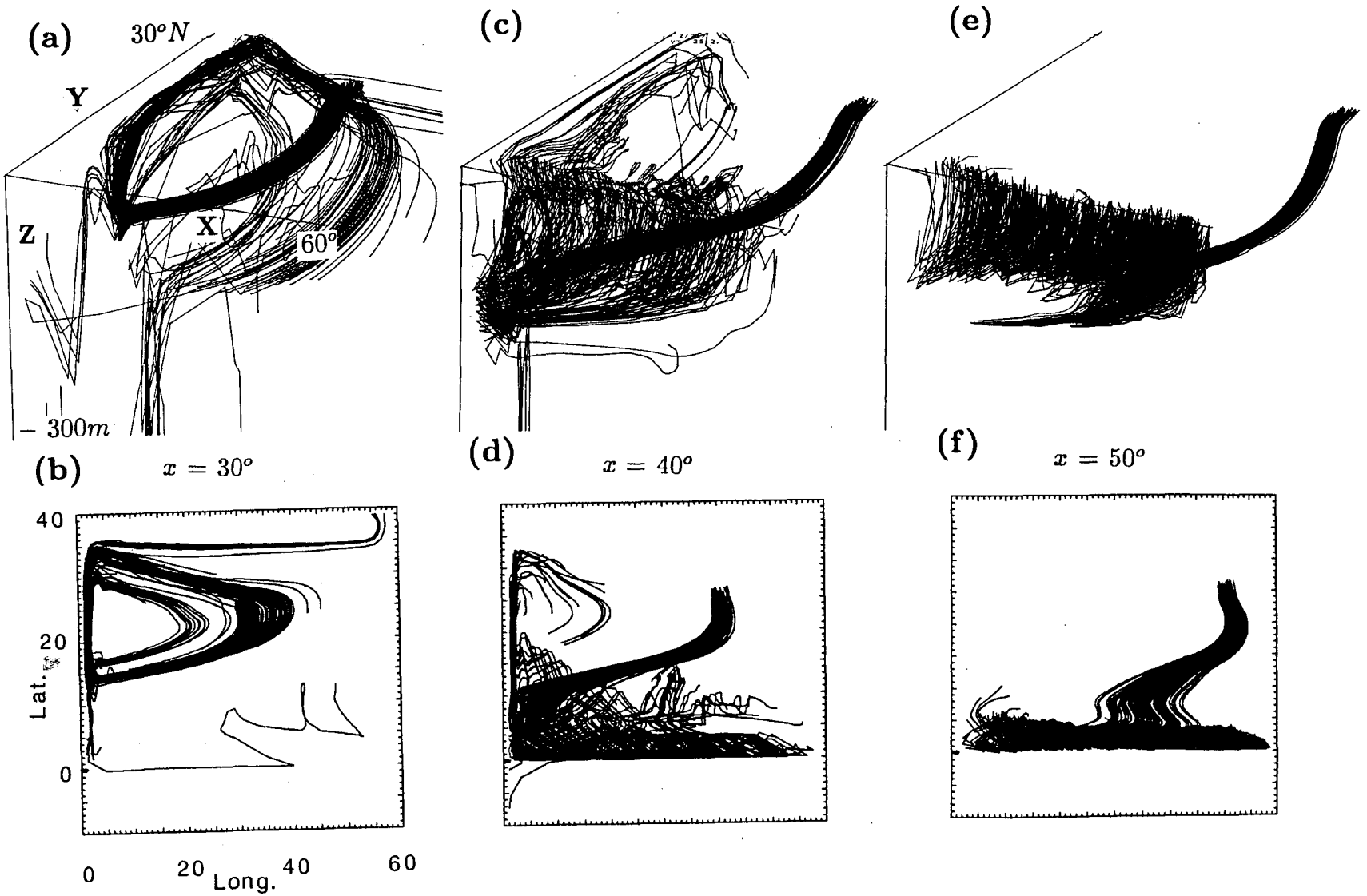

FIG. 7. The 3D view and plan of three types of trajectories illustrated by three groups of particles released on the surface at 26°N and followed for 10.5 years. (Each group has 100 particles initially distributed randomly on an area of 3° × 3°.) In (a) and (b), initial positions are centered at midbasin $x = 30°$, and most particles recirculate within the subtropical gyre. In (c) and (d), particles initially centered at $x = 40°$, travel equatorward through the low-latitude western boundary current. In (e) and (f), particles initially centered at $x = 50°$ flow equatorward through the oceanic interior.

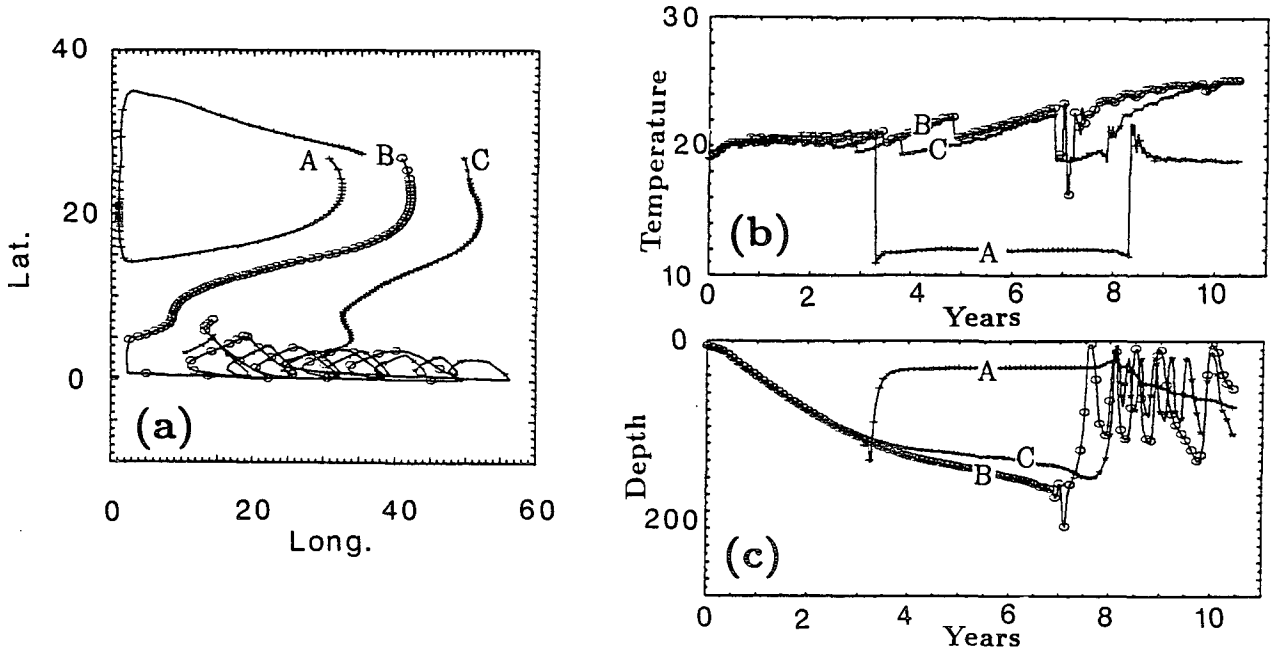

FIG. 8. (a) The top view of three typical trajectories, each in one group in Fig. 7. (b) and (c) The evolution of temperature and depth respectively, for the three particles in (a). Note the adiabatic subduction within the subtropical gyre between year 1 and year 5.

After year 8, particle A exits the midlatitude western boundary current, and recirculates back into the subtropical gyre.

2) SUBDUCTION WATER EXCHANGE WINDOW

To identify the exchange window, a more quantitative analysis on particle trajectories is carried out. Figure 9 describes some features of the subducted particles that start below the Ekman layer in the subtropical gyre. The contours in Fig. 9a show the minimum latitude that each particle reaches 13.5 years after being released. One critical contour is the one for particles that reach 12°N, which is indicated by the dot-connected line. A particle subducted at a position with a contour value smaller than 12°N has passed the southern boundary of the subtropical gyre and will eventually reach the equatorial region.[3] The particles subducted in the eastern part of the subtropical gyre within the area bounded by the 12°N contour, penetrate to the equatorial region. As shown in Fig. 9a, water subducted east of the 12°N contour (except in the region north of 25°N), flows as far south as 2°N. Thus the water does join the Equatorial Undercurrent. (See the particles in Figs. 7c–f and particles B and C in Fig. 8). This area therefore is the subduction region for the exchange water. Outside this region (in the western part of the subtropical gyre), subducted particles will recirculate within the subtropical gyre (like the particles in Figs. 7a,b and particle A in Fig. 8). This area is therefore the subduction region for recirculating water.[4]

Since outcrop lines in the subtropical gyre are predominantly in the zonal direction, each outcrop line can be divided into two windows. West of the 12° contour is the recirculating window. East of the 12° contour is the subduction mass exchange window, or simply the exchange window. These windows are labeled in Fig. 9c, which plots some critical contours.

The size of the windows vary on different outcrop lines, as indicated in Fig. 9c. The exchange window has a minimum width in the middle subtropical gyre and expands toward both the north and south. This mass exchange window agrees well with the simple theory in Liu (1994). The shape can be explained according to Eq. (3.1). In the middle subtropical gyre, the Ekman pumping is the strongest. So the window reaches its minimum size. Toward both sides, the Ek-

[3] It has been noticed that within the thermocline the latitude of splitting between the northward midlatitude western boundary current and the southward low-latitude western boundary current is always located at the southern boundary of the subtropical gyre 12° where the wind curl vanishes. The physics of the low-latitude western boundary current is not understood yet.

[4] The northern part is still uncertain because of the finite integration time for particles. If the time is long enough, more water will pass the southern boundary of the subtropical gyre and eventually reach the equator. In other words, in the northern part of subtropical gyre, the 12°N contour will expand, and the contour value of minimum latitude will decreases monotonically with time, approaching a steady state if the integration time is long enough.

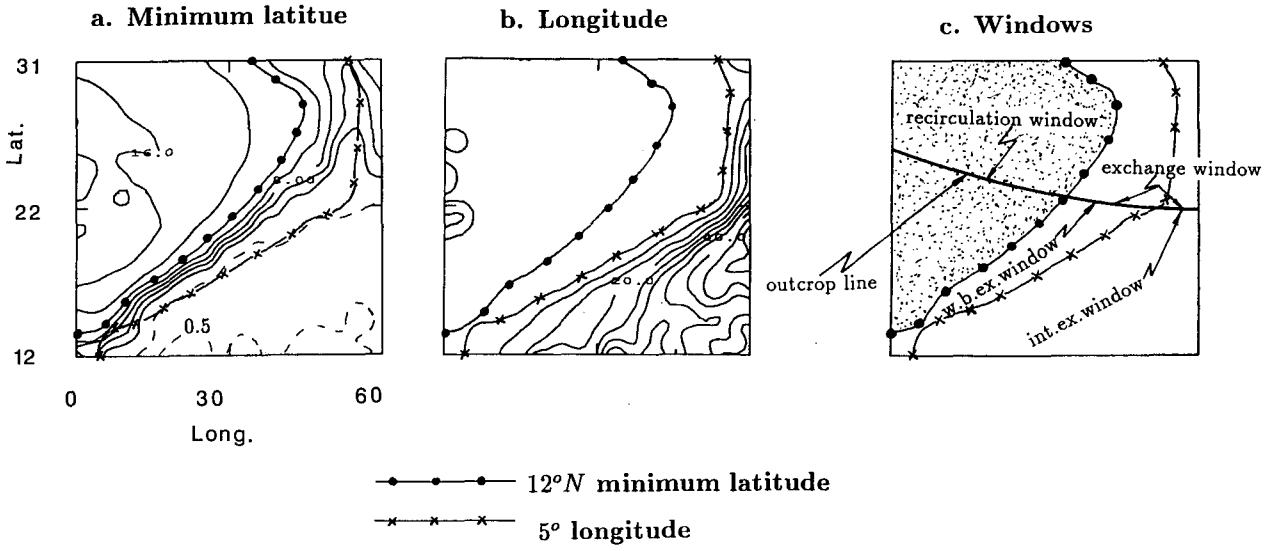

FIG. 9. The minimum latitude and the longitude that the subducted particles reach. The 2500 particles are released beneath the Ekman layer in the subtropical gyre ($z = 40$ m, $12°N < y < 32°N$). (a) The minimum latitude that each particle reaches (CI: 2°). The 0.5° minimum latitude is also drawn as a dashed line. (b) The longitude (CI: 10°) at which each particle reaches its minimum latitude in (a). The 5° contour is drawn as the cross-connected line. (c) Two critical contours and a typical outcrop line. The hatched area is the recirculation subduction region; the rest is the mass exchange subduction region. Windows on the outcrop line are also labeled. In (a)–(c), the two critical contours are the dot-connected line, which is the 12°N minimum latitude contour in (a), and the cross-connected line, which is the 5° longitude contour in (b).

man pumping decreases in its magnitude so that the window expands.

An important conclusion from the expansion of the window toward the north is the following: the amount of water that flows equatorward in the northern subtropical gyre is approximately the same as that in the southern subtropical gyre. [Remember that the window in the northern subtropical gyre has not expanded to its final state yet (see footnote 4).] This connection between the subtropical gyres is completely masked in the meridional streamfunction of Fig. 2c.

The origin of the subducted water that flows equatorward in the low-latitude western boundary current can be determined by recording at which longitude each particle reaches its minimum latitude. These longitudes are plotted in Fig. 9b. A particle subducted in an exchange window reaches the equator through the western boundary current provided the longitude in Fig. 9b is within 5° of the western boundary. We will regard the 5° contour in Fig. 9b (the cross-connected contour) as the critical contour that separates the two following regions: a western region with small contour values in which subduction particles reach their minimum latitude through the western boundary current, and an eastern region with large contour values in which subduction particles reach their minimum latitude in the interior of the ocean.

The 5° longitude contour are superimposed onto the minimum latitudes in Fig. 9a. On each outcrop line, the mass exchange window is further divided into two subwindows. East of the 12°N minimum latitude contour and west of the 5° longitude contour is the western boundary mass exchange subwindow; east of the 5° longitude contour is the interior mass exchange subwindow. The discussion of different windows is summarized as in Fig. 9c.

The window analysis in Fig. 9c agrees with the isothermal analysis in Fig. 3 and the trajectory paths in Figs. 7 and 9. Two features stand out. First, the water subducted in the western part recirculates within the subtropical gyre; further east, the water flows to the equator through the western boundary current (western boundary exchange subwindow); even further east, the water penetrates equatorward in the interior of the ocean (interior exchange subwindow). Second, for an outcrop line toward the southern boundary of the subtropical gyre, the interior exchange subwindow expands rapidly. It almost occupies the whole southern boundary of the subtropical gyre. In other words, most of the water subducted in the southern subtropical gyre tends to flow to the equator through the interior of the ocean. The opposite is true of the water that subducts in the northern part of the subtropical gyre.

Finally, by recording the time it takes each particle to reach the minimum latitude it is found that particles in the southern subtropical gyre reach the equator in about 3.5 to 6 years (consistent with Fig. 8). In addition, the water from the interior exchange window tends to reach the equator earlier (by several months or perhaps a year) than those from the west-

ern boundary exchange window. The reason is the longer distance that the latter group of particles travels.

b. Poleward flow of equatorial water

Water from the Equatorial Undercurrent flows poleward in three different ways. This can be seen in the trajectory projections on the X–Y plane as shown in Figs. 10a–c. Figure 10a shows the first path: it starts from above the core of the Equatorial Undercurrent and penetrates to the northern subtropical gyre by means of the surface western boundary current. Many particles first reach the southern subtropical gyre away from the western boundary (up to 10°) and continue eastward (by means of the subsurface geostrophic flow). Then, they subduct in the recirculating window region (see Fig. 9c) and are swept westward by the strong flow in the southern subtropical gyre. Finally they join the midlatitude western boundary current and penetrate to the northern subtropical gyre. Therefore, if one calculates the poleward flow in the western boundary as the transport within, say 5° of longitude, of the western boundary (as in Fig. 6), then the real western boundary transport toward the north will be seriously underestimated between 5°N and 12°N. This is why, in Fig. 6, the western boundary northward transport decreases abruptly from 4 to 1 Sv after crossing 5°N.

The second path can be seen in Fig. 10b, which shows particles starting from the upper core of the Equatorial Undercurrent. The water, after it surfaces, flows toward the southern subtropical gyre near the surface in the interior of the ocean. The projections on the Y–Z plane (not shown) are reminiscent of the subtropical cell shown in Fig. 2c.

The third path for water in the Equatorial Undercurrent starts in the lower part of that current's core. The projection of the trajectories on a horizontal plane is shown in Fig. 10c. These particles flow along the equator and upwell in the eastern ocean. After surfacing, they do not escape to the subtropics. Instead, they recirculate in the Y–Z plane within 5° of the equator, while drifting westward. This recirculation is seen more clearly in Fig. 11, which shows three typical trajectories. Figures 11a–c, show how, at the surface, the particles flow westward and poleward in the wind drift and Ekman drift. Then they downwell and converge on the equator as the subsurface geostrophic flow. They join the upper part of the Equatorial Undercurrent in which they resume their eastward and upward flow. The cycle continues with a net westward displacement each time, until the particles approach the western boundary and flow toward the subtropics through either the western boundary or the interior. The projection on the Y–Z plane in Fig. 11c shows clearly the equatorial cell of Fig. 2c: particles that recirculate in the upper 120 m.

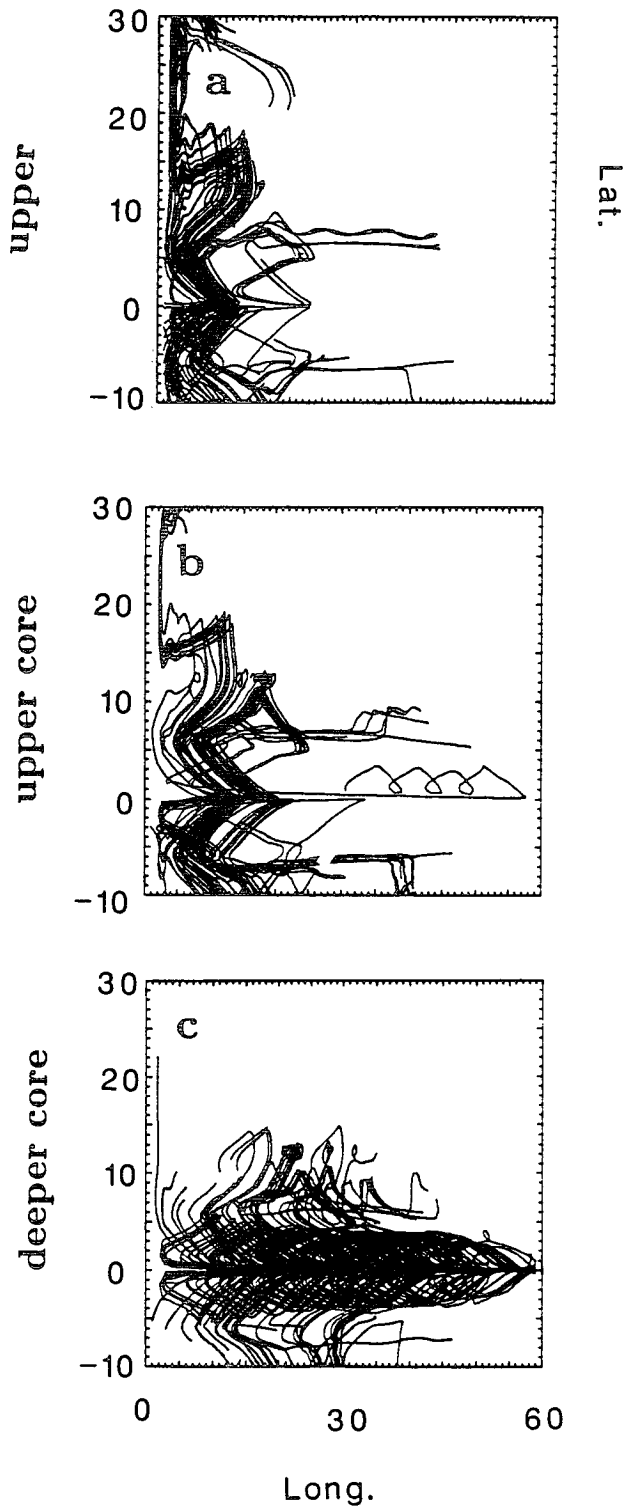

FIG. 10. Projection on a horizontal plane for trajectories of three subgroups of trajectories (each with 100 particles) three years after they are released in the Equatorial Undercurrent ($x = 10°$, $2°S < y < 2°N$). The three groups of trajectories are for particles in the Equatorial Undercurrent that start at depths between (a) 30 and 80 m above the core, (b) 80 and 130 m in the core, and (c) 130 and 180 m below the core.

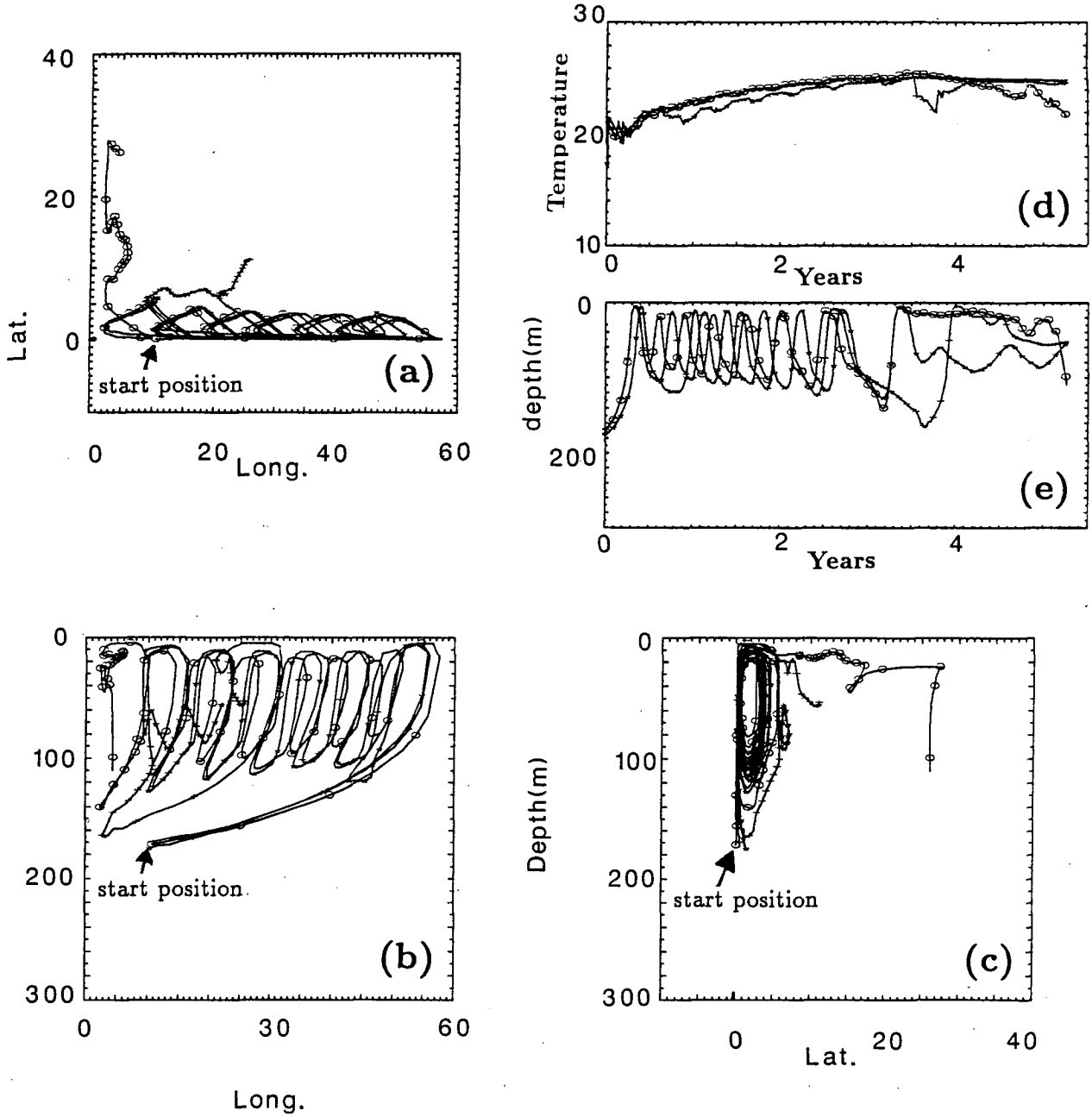

FIG. 11. (a)–(c) The projections of three particles that start in the core of the Equatorial Undercurrent. (d) and (e) The temperature and depth of the three particles as a function of time.

Although the maximum transport of the Equatorial Undercurrent in this case is 17 Sv (see Fig. 13), the two equatorial cells, one in each hemisphere, have transports of 50 Sv. Thus, on the average, each particle recirculates approximately three times before it exits to the subtropics. This is consistent with the results in Fig. 11. The time history of the temperature and depth in Figs. 11d,e further show that in the core of the Equatorial Undercurrent, particles flow almost adiabatically, consistent with observations (e.g., Bryden and Brady 1985) and some simple models (e.g., Pedlosky 1987). Later during the equatorial cell recirculation stage, particles are warmed more than 2°C while drifting westward. The eastward journey in the core takes about 3 months to cross the basin, whereas the circuitous westward journey in the upper ocean takes about 2 years with each cycle taking about 4 months.

5. The source water of EUC

a. *Tracking the source water of the Equatorial Undercurrent*

Figure 12a plots, as does Fig. 9b, the depth (solid line) and longitude at which subducted waters reach their minimum latitude. The depth contour is drawn only in the interior exchange subduction region that is located mainly in the southern part of the subtropical gyre. Since all particles subducted from this region join the Equatorial Undercurrent, we can take these depth contours as those of water parcels that reach the equatorial plane. Each longitude contour has a depth range in the southern subtropical gyre.

For example, the 10° contour almost coincides with the −120 m contour with a deviation of about 5 m. This means that the water subducted along the 10° contour in the southern subtropical gyre reaches the equator at 10° in the depth range of 115 and 125 m, in the upper core of the undercurrent. This is marked by the black bar at 10° of longitude in Fig. 12b. Similarly, one can identify the destination on the equator for the 20°, 30°, 40°, and 50° contours in Fig. 12a. (See the black bars in Fig. 12b.) From a mathematical viewpoint, we have mapped the subduction position in the southern subtropical gyre in Fig. 12a onto their destination on the equator in Fig. 12b.

The conclusion from Fig. 12 is that the water subducted within the interior exchange window in the southern subtropical gyre reaches the equator above the core of the Equatorial Undercurrent. It follows that the source water for the upper core of the Equatorial Undercurrent (roughly from 130–90 m in the west to 80–60 m in the east) comes from the southeastern subtropical gyre (in the interior exchange window).

This result plus our previous results concerning trajectories suggest that, in the upper Equatorial Undercurrent (roughly from 90–30 m in the west to 60–10 m in the east), the source water comes from the subduction region south of the subtropical gyre (5° to 12°N) and from the equatorial downwelling at the surface (3° to 5°N). The equatorial downwelling supplies water to the upper Equatorial Undercurrent. In and below the core of the undercurrent, the water comes mainly from the northeastern subtropical gyre and partly from the central basin in the southern subtropical gyre (in the western boundary exchange window). Notice that both source regions lie predominantly within the western boundary exchange region (see Fig. 12a). We therefore conclude that the water joins the core of the undercurrent mainly near the western boundary.

The above results suggest that a substantial amount of water joins the Equatorial Undercurrent in the west, by means of the low-latitude western boundary current. The next question is, how much?

Figure 13 shows the zonal transport of the upper ocean ($y < |5°|, z < 250$m) as a function of longitude. The eastward transport, which is mainly that of the Equatorial Undercurrent, is almost balanced by the westward transport in the upper ocean. The maximum transport, of about 17 Sv, is attained in the middle of the basin. The transport increases rapidly with distance from the western boundary and is already 14.5 Sv at

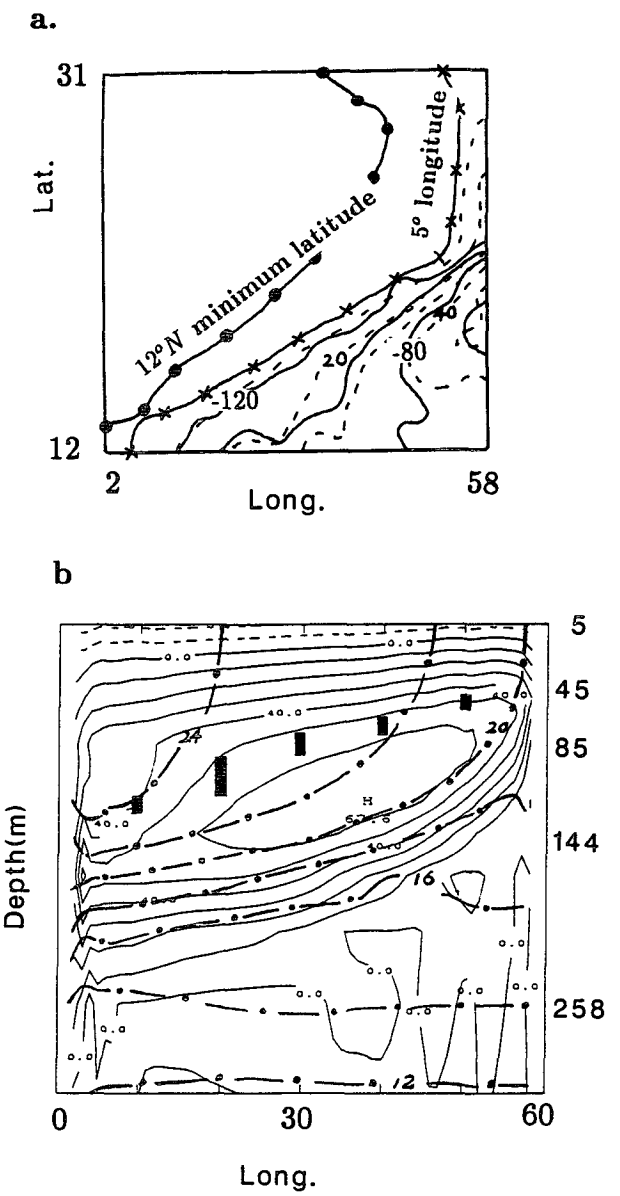

FIG. 12. (a) The depth (solid lines with a contour interval of 20 m) and longitude (dashed lines with a contour interval of 10°) at which each particle reaches its minimum latitude in Fig. 9a. The dot-connected line and the cross-connected line show the 12°N minimum latitude and the 5° longitude contours, respectively, as in Fig. 9. (The depth contours in the western boundary exchange subduction region are not shown.) (b) The zonal velocity (CI: 20 cm s^{-1}) and temperature (CI: 2°C) on the equatorial plane. The black bars along 10°, 20°, 30°, 40°, and 50° represent the destination of waters subducted in the interior exchange subduction region in the southern subtropical gyre as shown in the 10°, 20°, 30°, 40°, and 50° longitude contours in (a).

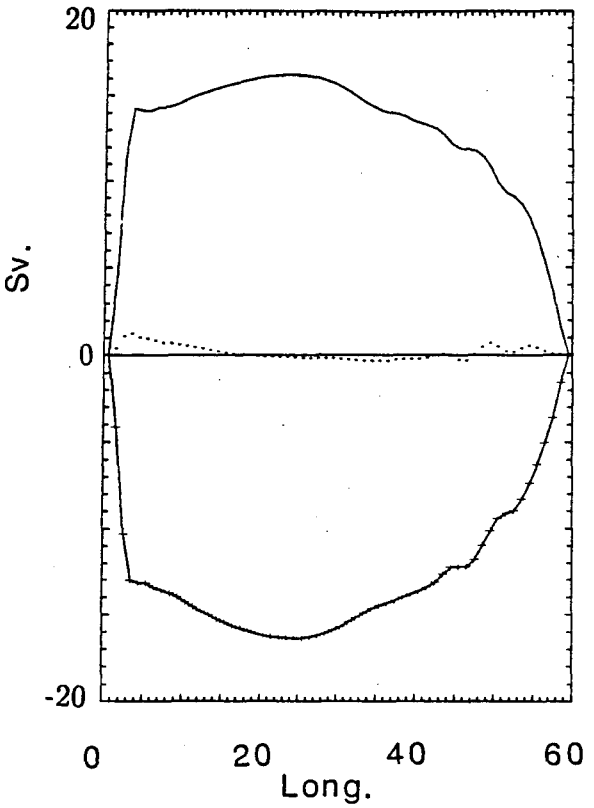

FIG. 13. The equatorial zonal transports within 5° of the equator. The dotted line is the net transport.

5° of longitude. This rapid increase means that most of the initial transport is supplied at the western boundary.

How much of this western boundary transport comes from the subtropical gyre? The reasoning in appendix A suggests that the western boundary current is sufficient to supply the initial transport of the undercurrent, which is not very different from its maximum transport. About two-thirds of the western boundary water comes from the subtropical gyre, primarily the northern subtropical gyre. The water from the northern subtropical gyre is important for the heat flux because of its low temperature.

b. *Source water of the Equatorial Undercurrent in the oceanic interior*

Water from the southern subtropical gyre, tropically subducted water, and local recirculated equatorial all join the Equatorial Undercurrent. In the western part of the basin these contributions cause the transport of the undercurrent to increase. To the east of the point of maximum transport the composition of the water in the undercurrent gradually changes. Upwelling removes water from the core at a rate that exceeds the influx at the depth of the thermocline.

Figure 12b shows that, in an eastward direction, the core of the Equatorial Undercurrent moves upward more slowly than does the thermocline. The reason is the local equatorial cell whose depth is independent of longitude as is evident in the trajectories of Figs. 11b,e. The mass contribution of this cell therefore keeps the depth of the core of the undercurrent approximately constant.

6. Concluding remarks

a. *Summary*

This article describes the flow field and particle trajectories in a model of the oceanic circulations in the subtropics and Tropics. Figure 14 is a schematic of these circulations. The Equatorial Undercurrent is seen to lose water in three ways. Water in the core surfaces in the eastern equatorial ocean and then circulates in the meridional plane while drifting westward within 5° of the equator. After the water reaches the surface layers of the western equatorial ocean, it can follow one of two poleward routes. One of them is through the oceanic interior, to a region of subduction equatorward of the latitude of zero wind stress. Thereafter the water returns equatorward to join the upper part of the Equatorial Undercurrent. In a meridional plane this corresponds to the subtropical cell. The other possibility is for a fluid parcel to travel to the northern subtropical gyre in a western boundary current. Subduction to deep isopycnals precedes equatorward flow that includes a journey in the deep, low-latitude, western boundary current.

The subtropical gyre has three subduction windows. The western one is the recirculating window, in which subducted waters recirculate within the subtropical gyre. To its east is the exchange window, in which subduction waters penetrate equatorward. This window can further be divided into two subwindows: the western boundary exchange window from which waters join the Equatorial Undercurrent through the western boundary current; and the eastern interior exchange window from which waters join the Equatorial Undercurrent through the oceanic interior. The southern part of the subtropical gyre is dominated by the interior exchange window, the northern part by the western boundary exchange window. When the subtropical wind curl vanishes, the exchange window expands substantially. On the other hand, if the tropical wind vanishes, the mass exchange window disappears and there is little exchange between the Tropics and subtropics. These results agree well with the theoretical work of Liu (1994).

The exchange transport, about 7 Sv in each hemisphere, is comparable to the transport of the undercurrent and is within 15% less than the Ekman transport at the equatorward boundary of the subtropical gyre, because the equatorward geostrophic flow is opposite to the Ekman drift.

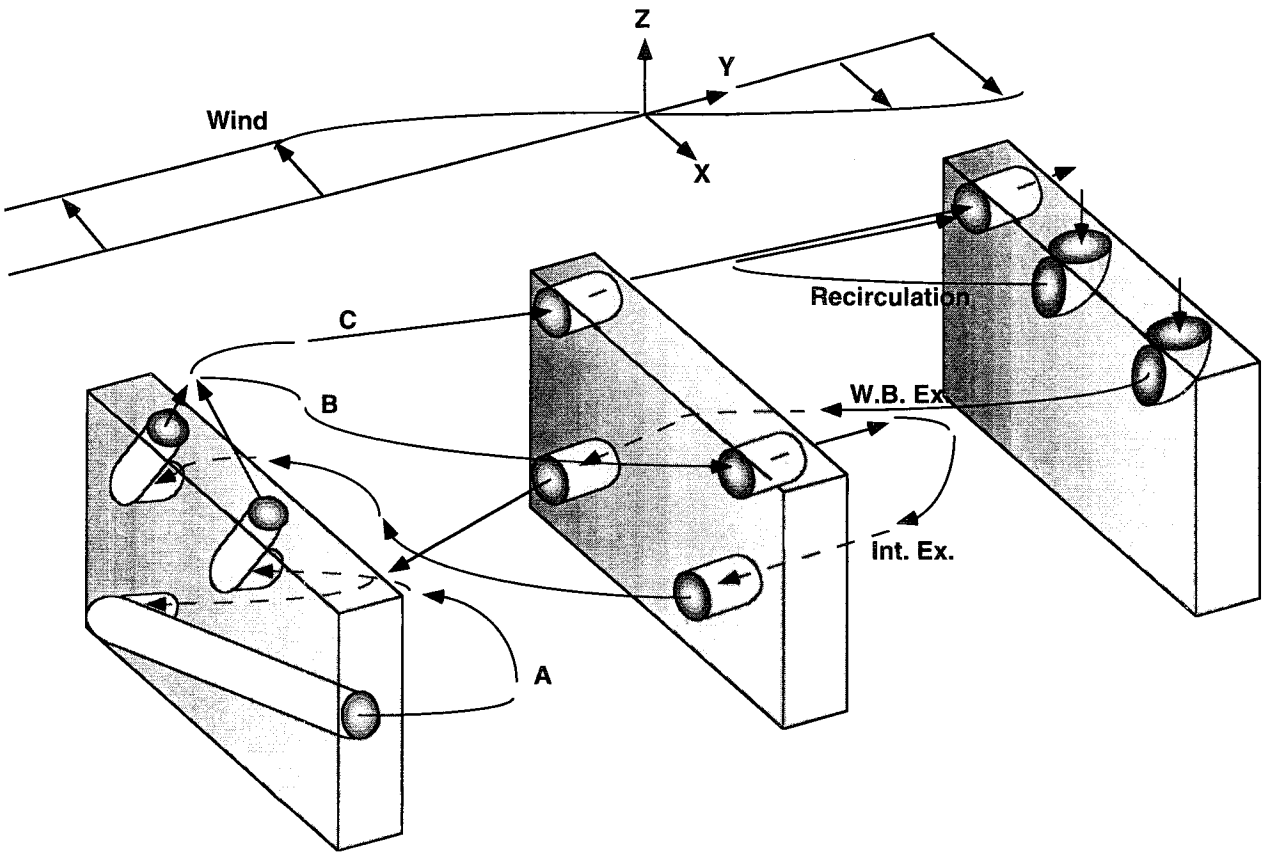

FIG. 14. A schematic that shows the circulation in a subtropical–tropical upper-ocean system. The wind stress is shown on the top left. The three branches correspond to the local equatorial cell (A), the interior mass exchange with the southern subtropical gyre (B), and the water exchange with the northern subtropical gyre (C).

About two-thirds of the water in the Equatorial Undercurrent in the west is supplied by the subtropical thermocline. Most of it originates in the northern subtropical gyre and reaches the equator by means of the low-latitude western boundary current. Water in the upper part of the undercurrent is partly recirculated locally, in the equatorial cell, and comes partly from the water subducted south of the subtropical gyre. Toward the east, the proportion of deep thermocline water in the undercurrent decreases as more and more upper thermocline water joins the EUC while the deeper thermocline water upwells into the surface.

b. Relevance to observations

The analyses of tritium data by Fine et al. (1987) indicate that tracer flows mainly through the oceanic interior to reach the Equatorial Undercurrent from the northern Pacific. This is consistent with the results from our model in which the water that subducts in the southern part of the subtropical gyre, which is occupied mostly by the interior exchange window, tends to penetrate equatorward through the interior of the ocean. The tracer analysis for the South Pacific tells a different story: middle and high latitude waters tend to join the Equatorial Undercurrent near the western boundary (Tsuchiya 1981; Tsuchiya et al. 1989; Toggweiler et al. 1989). This too is consistent with our results: water that subducts on the poleward side of the subtropical gyre, where there is essentially no interior exchange window, tends to join the EUC through the western boundary.

To facilitate analyses of the results, our model has been idealized in both its geometry and forcing. However, the simplifications preclude a detailed comparison of the results with observations. In further studies we propose to enhance the realism of the model by including a positive wind stress curl that drives a realistic North Equatorial Countercurrent (NECC). A strong eastward NECC can sweep the equatorward subsurface geostrophic flow eastward and can prevent the water from penetrating equatorward by means of the low-latitude western boundary current. McPhaden and Fine (1988) suggest that the NECC may be responsible for the equatorward penetration of tritium in the central North Pacific.

The other defect of the model that needs to be remedied is the coarse resolution along the western boundary. In Fig. 1, the midlatitude western boundary current

is clearly too viscous. This undoubtedly distorts the role that current plays in the exchange of water between the Southern Hemisphere and western equatorial Pacific (Tsuchiya et al. 1989).

Observations show a strong equatorial asymmetry in the flow patterns of both the Pacific and the Atlantic. In the Pacific, as discussed above, equatorward penetration occurs in midocean whereas, in the south, it occurs in the western boundary current. In the Atlantic, evidence for an asymmetry is less conclusive but seems to suggest a picture similar to that of the Pacific: the upper water of the equatorial Atlantic comes mainly comes from the South Atlantic subtropical gyre whereas the North Atlantic subtropical water is mostly blocked from the equatorial region, particularly in the interior ocean (Sarmiento et al. 1981; Kawase and Sarmiento 1985).

The asymmetry is in part caused by the asymmetry of the winds, which drive a countercurrent in one hemisphere only. Another factor is the strong thermohaline circulation in the Atlantic, which enhances the upper-ocean flow toward the north.

Acknowledgments. We are deeply indebted to Dr. J. Pedlosky for many discussions and suggestions. We appreciate discussions with Dr. P. Lu. We also thank Drs. K. Bryan, R. Toggweiler, and J. Sarmiento for useful conversations. Special thanks go to Ms. Koberle for assisting ZL in setting up the GCM. ZL was supported by the NOAA/UCAR postdoctoral fellowship in climate change. SGHP by NOAA Grant NA26GP0057. The computations were carried out on the CRAY-YMP at GFDL/NOAA.

APPENDIX

How Much of the Low-Latitude Western Boundary Transport Comes from the Subtropical Gyre?

Before answering the question, let us consider in detail the transport of the equatorward western boundary current in the thermocline of low latitudes. This transport is represented by the negative dash–dot line south of 12°N in Fig. 6. The transport shows two rapid increments toward the equator. They are caused by the convergence of westward and southward flow from the interior. At 12°N, the transport is at its minimum at less than 1 Sv. Farther south the transport increases rapidly to about 3 Sv at 5°N. This increase is supplied by water from the subtropical gyre because the water subducted south of 12°N flows eastward and therefore will not contribute to the enhanced western boundary transport. It follows that at least 6 Sv of subtropical water flows equatorward in the western boundary currents of the two hemispheres.

Equatorward of 5°N south the western boundary current exhibits a second increase to reach a maximum transport of 7 Sv at about 2°N. (This increase is caused partly by more subtropical thermocline water, partly by the tropical subducted water, subducted south of 12°N, and equatorial cell water downwelled between 3°N and 5°N.) Thus, the western boundary currents supply approximately 14 Sv to the EUC. This is consistent with the initial EUC transport at 5° (14.5 Sv). How much of this water comes from the subtropical gyres? As analyzed above, there are already 6 Sv of subtropical waters in the western boundary current at 5°. Farther south, even without tropical waters joining the western boundary current, there will be even more subtropical water converging onto the western boundary (in both upper and deeper thermocline). In this case, it seems reasonable to expect an increase in the western boundary current transport toward the equator similar to the increase that occurs between 12°N and 5°N. Linear extrapolation then gives a transport of about 5 Sv at 2°N. Thus we will expect about 10 Sv of subtropical water to join the EUC through the western boundary current. This is obviously consistent with the transport of the initial Equatorial Undercurrent core water, which accounts for about two-thirds of the initial EUC transport. The remaining part (about $14.5 - 10 = 4.5$ Sv) is then tropical water that joins the Equatorial Undercurrent above the core (above 80 m) at the western boundary either by subduction or by equatorial downwelling. Furthermore, it is important to point out that most of the subtropical water that joins the initial Equatorial Undercurrent comes from the northern subtropical gyre. Indeed, the water joining the Equatorial Undercurrent through the western boundary comes from the western boundary subduction window in the subtropical gyre (see Fig. 9c). This window mainly resides in the northeastern subtropical gyre. Thus, water from the subtropical gyre that joins the initial Equatorial Undercurrent comes primarily from the northern subtropical gyre. That gyre obtains its equatorial water mainly from the surface western boundary current, in which water always penetrates to the northern subtropical gyre. We can therefore estimate the returning northern subtropical water from the surface western boundary current. As seen in Fig. 6, the surface western boundary transport (positive dash–dot line) has a maximum transport of 3 Sv at 6°N. (See the discussion of Fig. 10a.) There is at least $2 \times 3 = 6$ Sv surface water penetrating to the northern subtropical gyre. Hence there is at least 6 Sv northern subtropical water returning to the equator. This return water comes mostly from the western boundary because the interior exchange window is small in the northern subtropical gyre.

REFERENCES

Bryan, K., 1969: A numerical method for the study of the circulation of the World Ocean. *J. Comput. Phys.*, **4**, 347–376.

Bryden, L. H., and E. C. Brady, 1985. Diagnostic model of the three-dimensional circulation of the upper equatorial Pacific Ocean. *J. Phys. Oceanogr.*, **15**, 1255–1273.

Fine, R. A., W. H. Peterson, and H. G. Ostlund, 1987: The penetration of tritium into the tropical Pacific. *J. Phys. Oceanogr.* **17,** 553–564.

Kawase, and J. L. Sarmiento, 1985: Nutrients in the Atlantic thermocline. *J. Geophys. Res.*, **90,** 8960–8979.

Liu, Z., 1994: A simple model of the mass exchange between the subtropical and tropical ocean. *J. Phys. Oceanogr.*, **24,** 1153–1165.

——, and S. G. H. Philander, 1994: The response of the tropical–subtropical thermocline circulation to different wind forcing. *J. Phys. Oceanogr.*, **24,** submitted.

McCreary, J., 1985: Modeling equatorial ocean circulation. *Annu. Rev. Fluid Mech.*, **17,** 359–409.

——, and Z. Yu, 1992: Equatorial dynamics in the 2.5 layer model. *Progress in Oceanography,* Pergamon.

——, and P. Lu, 1994: On the interaction between the subtropical and equatorial ocean circulations: The subtropical cell. *J. Phys. Oceanogr.*, **24,** 466–497.

McPhaden, M. J., and R. A. Fine, 1988: A dynamical interpretation of the tritium maximum in the central equatorial Pacific. *J. Phys. Oceanogr.*, **18,** 1454–1457.

Munk, W. H., 1950: On the wind-driven ocean circulation. *J. Meteor.*, 7, 79–93.

Pacanowski, R. C., and S. G. H. Philander, 1981: Parameterization of vertical mixing in numerical models of tropical oceans. *J. Phys. Oceanogr.*, **11,** 1443–1451.

——, K. W. Dixon, and A. Rosati, 1991: The GFDL Modular Ocean Model users guide. GFDL Ocean Group Tech. Rep. No. 2.

Pedlosky, J., 1987: An inertial theory of the Equatorial Undercurrent. *J. Phys. Oceanogr.*, **17,** 1978–1985.

——, 1991. The dynamics of subtropical ocean circulation. *Science.*

Philander, S. G. H., 1990: *El Niño, La Niña and the Southern Oscillation.* Academic Press, 293 pp.

——, and R. C. Pacanowski, 1980: The generation of equatorial currents. *J. Geophys. Res.*, **85,** 1123–1136.

Rhines, P., 1986. The vorticity dynamics of ocean circulation. *Annu. Rev. Fluid Mech.*, **18,** 433–447.

Semtner, A. J., and W. R. Holland, 1980: Numerical simulation of equatorial ocean circulation. Part I. A basic case in turbulent equilibrium. *J. Phys. Oceanogr.*, **10,** 667–693.

Sarmiento, J. L., C. G. H. Rooth, and W. Roether, 1981: The North Atlantic tritium distribution in 1972. *J. Geophys. Res.*, **87,** 8047–8056.

Toggweiler, R., K. Dixon, and W. S. Broecker, 1989: The Peru upwelling and the ventilation of the South Pacific thermocline. *J. Geophys. Res.*, **96,** 20 467–20 497.

Tsuchiya, M., 1981: The origin of the Pacific 13°C water. *J. Phys. Oceanogr.*, **11,** 794–812.

——, R. Lukas, R. A. Fine, E. Firing, and E. Lindstorm, 1989: Source waters of the Pacific Equatorial Undercurrent. *Progress in Oceanography,* Vol. 23, Pergamon, 101–147.